

Precision hfs of $^{126}\text{Cs}(T_{1/2}=1.63\text{m})$ by ABMR

J. Pinard¹⁾, H.T. Duong¹⁾, D. Marescaux¹⁾, H.H. Stroke²⁾, O. Redi²⁾, M. Gustafsson³⁾, T. Nilsson³⁾, S. Matsuki⁴⁾, Y. Kishimoto⁴⁾, K. Kominato⁴⁾, I. Ogawa⁴⁾, M. Shibata⁴⁾, M. Tada⁴⁾, J.R. Persson⁵⁾, Y. Nojiri⁶⁾, S. Momota⁶⁾, T.T. Inamura⁷⁾, M. Wakasugi⁷⁾, P. Juncar⁸⁾, T. Murayama⁹⁾, T. Nomura¹⁰⁾, M. Koizumi¹¹⁾ and ISOLDE Collaboration^{??)}

Abstract

A precision measurement of the $^{126}\text{Cs}(T_{1/2}=1.63\text{m})$ hfs separation $\Delta\nu$ in the ground $6s\ ^2S_{1/2}$ state was obtained by means of atomic beam magnetic resonance on-line with the CERN-PSB-ISOLDE mass separator. The result is $\Delta\nu=3629.514$ (0.001)MHz. The ultimate goal is a systematic study of the influence of extended nuclear structure on hfs (Bohr-Weisskopf effect). These hfs data can serve to gain knowledge of neutron distributions, of recent interest in nuclear astrophysics and parity non-conservation effects in atomic interactions.

Submitted to Physical Review A

-
- ¹⁾ Laboratoire Aimé Cotton, CNRS II, Bât 505, Faculté des Sciences, F91405 Orsay Cedex, France
²⁾ Department of Physics, New York University, 4 Washington Place, New York, NY 10003, USA
³⁾ Department of Physics, Chalmers University of Technology, S-41296 Göteborg, Sweden
⁴⁾ Nuclear Science Division, Institute for Chemical Research, Kyoto University, Gokasho, Uji-shi, Kyoto, 611-0011, Japan
⁵⁾ Högskolan Kristianstad, SE-291 88 Kristianstad, Sweden
⁶⁾ Laboratory of Pure- and Applied Physics, Kochi University of Technology, Tosayamada, Kochi 782-0041, Japan
⁷⁾ Accelerator Research Facility, RIKEN, Wako-shi, Saitama, 351-0198, Japan
⁸⁾ Institut National de Métrologie du CNAM, 292 rue St. Martin, F-75141 Paris Cedex 03, France (unité associée au CNRS: URA 827)
⁹⁾ Tokyo University of Mercantile Marine, 2-1-6 Etchujima, Koto-ku, Tokyo, 135-0044, Japan
¹⁰⁾ Institute of Particle and Nuclear Studies, High Energy Accelerator Research Organization, 1-1 Oho, Tsukuba, Ibaraki 305-0801, Japan
¹¹⁾ Japan Atomic Energy Research Institute (JAERI), Shirakata Shirane 2-4, Toikaimura, Naka, Ibaraki 319-1195, Japan
¹²⁾ CERN, 1211 Geneva 23, Switzerland

1 Introduction

The combination of precise hfs and nuclear g -values can reveal the influence of the distributed nuclear magnetization on hfs- the *hfs anomaly* or *Bohr-Weisskopf effect* (BW). We have described previously [1] the atomic beam magnetic resonance (ABMR) apparatus to measure each to an accuracy of 10^{-5} or better. Precision measurements of the hfs represent a first important and necessary step in determining BW and its systematic study in an isotopic chain. The principles of the measurements were also described as were successful hfs and g -value experiments on stable K and Rb [1]. The apparatus is an evolution from our earlier hfs work on radioisotopes that combined ABMR with laser optical pumping[2].

A prime motivation for studying BW is that it gives insight into isotopic variations of the neutron distribution in nuclei. This is important in the interpretation of studies of isotopic variations of parity nonconservation (PNC) in atomic interactions[3][4], an alternative to precise single isotope studies but in different atomic transitions[5]. PNC has in fact been suggested [6] as a possible source of information on neutron distributions. Neutron star structure and its relation to neutron radii and distributions[7] has also been pointed out as an area of application of BW. Further, precision hfs, nuclear g -factor, and BW measurements are required in the interpretation of the hfs of hydrogenic ^{209}Bi (Bi^{82+}) obtained in the storage ring at GSI, Darmstadt[8]: the extraction of QED effects and nuclear structure information rely on such knowledge[9].

In spite of this interest in neutron distributions, atomic hfs and nuclear multipole moments provide one of few means to obtain them. We have shown[10] with the use of nuclear configuration mixing theory of Arima and Horie[11], extended to include the effect of distributed nuclear magnetization, that the combination of nuclear magnetic moment and BW data can serve to obtain information on nuclear wave functions and on isotopic neutron variations.

The apparatus[1] was moved to CERN for work with short-lived radioactive cesium isotopes "on-line" produced with use of the PSB (proton-synchrotron booster) - ISOLDE mass separator. We encountered unexpected production problems: First, ISOLDE furnishes 60-keV ion beams. These have to be neutralized and *thermalized*, so that simple, efficient, charge exchange cells cannot be used, as we do in collinear laser spectroscopy[12]. The rate of radioactive ions produced by ISOLDE is a limitation, but this was anticipated: the signal-to-noise ratio limits severely the precision of the measurements compared to one obtainable with stable isotopes. We report our first measurement performed on line, $\Delta\nu$ (^{126}Cs), with the use of this apparatus, modified for radioactive isotope studies.

2 Magnetic dipole hfs interaction

In the cesium ground state the electron angular momentum $J = 1/2$; the two total angular momentum states $F_+ = I + 1/2$ and $F_- = I - 1/2$ are separated by an energy ΔW . I is the nuclear spin and equals 1 for ^{126}Cs . One obtains readily $\Delta W/h = a(I + 1/2) \equiv \Delta\nu$, where $\Delta\nu$ is the hfs separation in frequency units, h Planck's constant, a the magnetic dipole hfs interaction constant. The latter was calculated for a point nucleus by Fermi and Segrè [13]

$$a_{pt} = \frac{16\pi}{3} g\mu_B^2 |\psi(0)|^2 \frac{m}{M}, \quad (1)$$

$\mu_I = gI\mu_N$, μ_I is the nuclear magnetic dipole moment in Bohr magnetons, g the dimensionless nuclear g -factor, the nuclear magneton $\mu_N = \mu_B(m/M)$, μ_B the Bohr magneton, m , M electron and proton masses, $|\psi(0)|^2$ the electron probability at the origin (nucleus). For the nucleus with extended electrical charge and magnetization distributions, Eq.(1) has to be modified accordingly. We write formally for the experimental a , $a_{exp} = a_{pt}(1 + \varepsilon_{BW})(1 + \varepsilon_{BR})$. The modification

in the magnetic dipole interaction, ε_{BW} , is BW. The finite charge distribution modifies the electron wavefunction from the one corresponding to the Coulomb potential of a point charge. This leads to the Breit-Rosenthal (BR) correction, ε_{BR} to a_{pt} [9]. In cesium ε_{BR} is small, so that $a \approx a_{pt}(1 + \varepsilon_{BW})$. Ideally one would extract $\varepsilon_{BW} = \frac{a}{a_{pt}} - 1$. This is possible for muonic atoms where one can calculate a_{pt} neglecting the atomic electrons. For ordinary atoms, we can only seek the variation between isotopes 1 and 2. Taking to a good approximation $\left(\frac{a_1}{a_2}\right)_{point} \approx \frac{g(1)}{g(2)}$ and, as in earlier cesium experiments[14] ε small, one obtains

$$\left(\frac{a_1}{a_2}\right)_{exp} \left[\frac{g(2)}{g(1)}\right] - 1 = \varepsilon_{BW}(1) - \varepsilon_{BW}(2) \equiv {}^1\Delta^2. \quad (2)$$

Bulk NMR is not possible with the quantities of radioisotopes produced and one has to rely on the Zeeman effect of the hfs to obtain the nuclear g -values. Alternatively, but not completely equivalent, Grossman *et al.* [15] obtain $(a_1/a_2)_{point}$ from an atomic state for which the valence electron has a smaller probability at the origin. (Examples of the dependence of Δ on atomic states can be found in [10].) Persson[16] discusses the possibility of obtaining $(a_1/a_2)_{point}$ by isolating the contact and non-contact contributions in the analysis of the hfs, *i.e.* the parts that are respectively sensitive or not to the extended nuclear structure. The hfs energy $W(F, m_F)$ is given by the well-known Breit-Rabi equation [17] in terms of the field parameter $x \equiv (g_J - g_I) \frac{\mu_B B}{h \Delta \nu}$. \mathbf{B} is the magnetic field. The nuclear Landé g -factor is defined as $g_I \equiv -\mu_I$ (in Bohr magnetons)/ $I = -\mu_I$ (in nuclear magnetons)(m/M)/ $I = -g(m/M)$. The resulting Zeeman pattern for ^{126}Cs ($I=1$) is shown in Fig. 1. Transitions $\Delta F = F_+ - F_- = 1$, $\Delta m_F = \pm 1$, were observed at very low B ($x \ll 1$). By expanding the Breit-Rabi formula to second order in x , we obtain

$$\frac{\Delta W}{h} \approx -\frac{\Delta \nu}{2(2I+1)} + g_I \mu_B B m_F \pm \frac{\Delta \nu}{2} \left\{ 1 + \frac{2m_F x}{2I+1} + \frac{x^2}{2(2I+1)^2} [(2I+1)^2 - 4m_F^2] \right\}, \quad (3)$$

from which one can deduce the frequency of each of the four rf lines of the observed structures. The signs \pm are respectively for F_+ and F_- . For a precise determination of g_I , a large B -value is required to measure the direct term $g_I \mu_B B m_F$.

3 Experimental method

The apparatus described in [1] includes the triple rf loop magnetic resonance setup for direct g_I measurement; for the purpose of this experiment only the C loop was used. Modifications for the on-line work with radioactive isotopes include a first hexapole focussing magnet and an auxiliary ion beam source for off-line extended testing: they are described in [9]. An oven containing stable ^{133}Cs ($\text{CsCl} + \text{K}$ or Na , heated to ≈ 200 °C) could also be inserted as a beam source for alignment purposes and for setting the frequencies of the lasers to the cesium resonance lines. This beam could be detected with use of a retractable conventional 2-mm wide iridium surface-ionization detector or by atom fluorescence.

The ion beam from ISOLDE is first sent through a neutralizer to get, at the output, a thermal beam of neutral atoms; this device proved to be the most critical one of the whole apparatus and is described separately. The beam of neutrals then passes through the first hexapole used as a focussing magnet to increase the transmission of the apparatus for the atoms in the $m_J = +1/2$ magnetic substate (low field seeker state) of the ground atomic state. This acts as a selector of the $F = I+1/2$ hfs levels shown in Fig. 1. After crossing the interaction region, these atoms are detected using a second hexapole magnet which focuses the $m_J = +1/2$ atoms on the entrance of the ionizer of a mass spectrometer (MS). This allows us to selectively detect

the radioactive atoms of interest and avoid background due to the stable elements produced by the ionizer and neutralizer. After crossing the first hexapole magnet, the atoms are optically pumped into the $^2S_{1/2}$ ($F=1/2$) level with use of a laser diode whose frequency is tuned to the $^2S_{1/2} \rightarrow ^2P_{3/2}$ ($F = 3/2$) transition. The atoms in the $^2S_{1/2}$ ($F = 1/2$) state are then defocused by the second hexapole magnet and the signal of the MS falls to zero, which enables us to work on a zero background to increase the detection sensitivity. When the rf field is applied, at resonance all the atoms may be transferred back to the $^2S_{1/2}$ ($F = 3/2$) level (depending on the rf power) producing the reappearance of the MS signal. A Hall probe, introduced as close as possible to the rf loop, allowed us to control the residual magnetic field. The field is set to zero using a small current in the electromagnet. Nevertheless, as can be observed in Fig. 2, a small inhomogeneous B -field still exists in the interaction region, but its effect on our measurements is negligible.

Before entering the second hexapole magnet, the atomic beam crosses a fluorescence detection region; this allows us to detect the population of the $^2S_{1/2}(F=3/2)$ level through laser-induced fluorescence using the recycling transition $^2S_{1/2}(F=3/2) \rightarrow ^2P_{3/2}(F=5/2)$. This alternative method, used in [1], looked also very promising: however, the existence of a background, due to laser stray light at the same wavelength as the fluorescence, does not permit the detection of the signal in the case of a very weak atomic beam.

The optical pumping as well as the fluorescence signal are induced with use of a single mode laser diode, Model SDL-5401-G1, which can provide up to 50 mW in the 850-nm region. Its frequency is stabilized on the band pass of a stable confocal etalon using a servo loop. The frequency is tuned by acting on a rotating galvo plate inserted in the etalon cavity close to the Brewster angle. The frequency stayed tuned to the atomic resonance for periods of hours .

The ^{126}Cs was produced by bombardment of a molten lanthanum target with 1.4-GeV protons from the PS Booster. The nominal yield is 6.9×10^{10} ions/s[18]. At the ABMR apparatus we had 10^{10} . In earlier experiments [19] the 60-keV ion beam was successfully thermalized and neutralized with an S-shaped, square cross-section tantalum neutralizer coated with yttrium. It is described in detail in [20]. In our first radioactive beam trial the thermalization and neutralization, however, proved inadequate. It was not clear whether this was due to the yttrium deposition process, its possible oxidation, or operating conditions ($\approx 1200^\circ\text{C}$).

A number of tests were made with the earlier types of neutralizers. For instance, low work function thoriated tungsten was tested, but the excessive stable cesium background precluded its use. We obtained the best result with an adaptation of the "orthotropic" neutralizer conceived by Dinneen, Ghiorso, and Gould[21]. It is basically a heated cylindrical tantalum box with a hole to admit the Cs^+ beam from ISOLDE. An yttrium electrode at $\approx -100\text{V}$ attracts the ions: if neutralized, they can bounce around and escape through a small exit hole, if not the ions can be reattracted to the yttrium to try again. Unlike our previous designs where ions had essentially one chance to get neutralized/thermalized, here they can be reused. Nevertheless, the efficiency of the system was certainly not proved to be optimized either as to materials or operating temperatures. The simulation calculation allowed an estimate of $\sim 10^{-3}$ as an upper limit of the neutralizer efficiency. We found in subsequent off-line tests that the desorption time constant of cesium ions implanted at 30 keV in tantalum is more than 10 s and that good desorption efficiency requires a temperature around 2000°C . This was not possible with our system. We also showed that the use of rhenium instead of tantalum has substantial advantages at the same temperature: lower desorption time constant and much better efficiency. Tests at this energy are also much more realistic for work with the ISOLDE ion beam.

The 240-cm long trajectory of the atoms in the beam is mainly governed by the two hexapole magnets located between the neutralizer and the ionizer at the entrance of the MS.

The first hexapole is a permanent magnet 16 cm long with an aperture 16 mm in diameter. With the use of a small Hall probe, measurements of the field along a diameter showed that it can be well approximated by a quadratic relation: B (in G) = $190 r^2$, where r is the distance from the axis in mm. This magnet is in a mechanical mount which allows its displacement over 10 cm along the atomic beam axis. The entrance face of this first hexapole was set at ≈ 30 cm from the neutralizer. The second hexapole is an electromagnet 45 cm long, 14 mm aperture diameter. The field on the poles can be adjusted up to 1 T. with optimum MS signal found at 0.8T. To study and optimize the transmission of the apparatus, we performed atom trajectory simulations using the SIMION software [22]. Assuming a Maxwellian velocity distribution corresponding to a neutralizer temperature of 1800°C , we found a transmission efficiency of the order of 10^{-5} from the exit of the neutralizer to the re-ionization "hot wire" of the MS. If, on the other hand, we optically pump the atoms in the intermediate region, changing the magnetic substate from a "low-field seeker" to a "high-field seeker", the number of atoms arriving on the MS did not fall to zero: there remained a residual signal which reached up to 10 percent of the full transmission depending on the temperature of the source. The simulation also showed that the assembly of the two hexapole magnets acted as an effective velocity filter, which can account for the shape of the resonance lines shown in Fig. 3. We discuss this in IV: it did not affect the precision of the determination of $\Delta\nu$.

The homogeneity of the C field is about 5×10^{-6} at a field of 0.65 T[1]. For $B \approx 0$, where our experiments were done, the remnant fields are expected to degrade this value. The single rf loop, also depicted in [1], is 2 cm wide, and the rf field is perpendicular to the C field. The rf was provided by a frequency synthesizer, Hewlett-Packard Model 83731B, coupled to an rf amplifier. During the recording, the frequency was scanned by steps with a minimum of 1 kHz per step. Between each step the ion signal was integrated for 5 or 10 seconds.

4 ^{126}Cs hfs measurement and results

Figure 2 shows the MS signal *vs* the rf frequency. The narrow resonance line corresponds to the two magnetic transitions F, m_F $(1/2, -1/2) \rightarrow (3/2, 1/2)$ and $(1/2, 1/2) \rightarrow (3/2, -1/2)$. From (3) these are $\delta\nu_{\pm} = \Delta\nu \pm g_I\mu_B B + (4/9)\Delta\nu x^2$, first order independent of x . The two broad separated resonances correspond to transitions $(1/2, -1/2) \rightarrow (3/2, -3/2)$ and $(1/2, +1/2) \rightarrow (3/2, 3/2)$, $\delta\nu_{\pm} = \Delta\nu \pm g_I\mu_B B \pm (2/3)\Delta\nu x + (2/9)\Delta\nu x^2$, and depend linearly on x . From their relative positions and widths one can estimate the residual magnetic field and its homogeneity: the magnetic field splitting $(8/3)\mu_B B \approx 1$ MHz (Fig. 2) giving for the residual magnetic field $B \approx 0.27$ G ($x \simeq 2 \times 10^{-4}$). From this value we can estimate the splitting between the two components of interest as well as their shift with respect to the exact value $\Delta\nu : 2g_I\mu_B \cong 0.4$ kHz, $(4/9)\Delta\nu x^2 \cong 8 \times 10^{-2}$ kHz.

As expected, and shown in Figs. 2 and 3, the background is not zero: it corresponds to 8 counts/s, 5 of which come from the ionizer of the MS itself. The remaining counts may be attributed to the efficiency of the optical pumping and the selectivity of the hexapole magnet. Fig. 3 shows two recordings of the main rf resonance signal with 5- and 10-s integration times per step. The two recordings are obtained at different rf power levels, spectrum a) at the higher one. The resonance evidently exhibits saturation, characteristic of the transition probability, P , ("Rabi oscillation" of population) as the rf power is increased. This is understood with use of the result for P as a function of the rf perturbation strength, as given by Ramsey[23], in which we replace the interaction time t by L/v (L , rf interaction length, v atomic velocity). There is a velocity selection produced by the two hexapole magnets. With a monoenergetic atomic beam and at sufficiently high rf power, modulations in the Lorentzian shape resonance curve appear, the center becoming either a maximum or a minimum, depending on the rf power. The line

shape structure is smoothed or disappears after integration over a velocity distribution.

We analyzed the data with use of different fitting programs. The result of a Gaussian fit is shown in Fig. 3. Our final result is

$$\Delta\nu(^{126}\text{Cs}) = 3629.514(0.001)\text{MHz}.$$

This is in agreement with our less precise value 3632.1(4.2) by laser spectroscopy[24], but differs significantly from the result 3640.8(39) quoted in [25]. As shown in IV, the precision of our result is not affected by uncertainties in B . The experiment[25] was done with B up to 213 G, measured by observing hfs resonances in a beam of ^{39}K . The Breit-Rabi formula shows that the corresponding hfs transition frequencies in ^{126}Cs (see Table 2 in [25]) depend on g_I and provide, in principle, the possibility of determining the hfs anomaly $^{133}\Delta^{126}$, Eq.(2). An attempt was made to extract from all these measurements a first estimate of $^{133}\Delta^{126}$: with use of the precise values of $\Delta\nu(^{126}\text{Cs})$ and of $g_J(\text{Cs})$, the value of $\mu_B B$ as given in [25], and the nuclear g -value of ^{126}Cs as a free parameter, we obtain $\mu(^{126}\text{Cs}) = 1.21 \mu_N$. From the known values of the stable isotope $\Delta\nu(^{133}\text{Cs})$ and $g_I(^{133}\text{Cs})$, and the assumption $^{133}\Delta^{126} = 0$ in (2), we obtain $\mu(^{126}\text{Cs}) = 0.77\mu_N$. The discrepancy between these values for $\mu(^{126}\text{Cs})$ is much too large to be accounted for by a reasonable hfs anomaly (usually \sim fraction of a percent, or less). It has been suggested that a possible source of error in [25] is the calibration of the magnetic field, but this was not controllable in our fitting procedure: we thus cannot rely on the measurement of $g_I(^{126}\text{Cs})$ [25] performed in the magnetic field for the determination of BW.

The ABMR method, with which we have measured earlier BW of longer-lived cesium isotopes off-line, has the advantage of a continuous beam: we have shown here the possibility of extending our studies to very short-lived isotopes on-line. While the beam technique cannot be applied to ions, we mention in closing that the use of ion traps has been suggested for determining BW[26]; no results appear to date.

HHS, JP, HTD thank NATO for Collaborative Research Grant CRG 951383. One of us (HHS) thanks Maurizio Pieve (Pisa) for system documentation and Claire Tamburella (CERN) for help with the experiment.

References

- [1] H.T. Duong *et al.*, Nucl. Instrum. Methods A **325**, 465 (1993).
- [2] H.T. Duong *et al.*, J. Phys. (Paris) **43**, 509 (1982); H.T. Duong *et al.*, J. Phys. (Paris) **47**, 1903 (1986).
- [3] E.N. Fortson, Y. Pang, L. Wilets, Phys. Rev. Lett. **65**, 2857 (1990).
- [4] A.-M. Mårtensson-Pendrill, Phys. Rev. Lett. **74**, 2184 (1995).
- [5] C.S. Wood *et al.*, Science **275**, 1759 (1997).
- [6] C.J. Horowitz *et al.*, Phys. Rev. C **63**, 025501 (2001).
- [7] C.J. Horowitz, J. Piekarewicz, Phys. Rev. Lett. **86**, 5647 (2001), Phys. Rev. C **64**, 062802(R) (2001).
- [8] I. Klaft *et al.*, Physica Scripta **T59**, 211 (1995).
- [9] H.H. Stroke, H.T. Duong and J. Pinard, Hyperfine Interactions **129**, 319 (2000).
- [10] H.H. Stroke, R.J. Blin-Stoyle, V. Jaccarino, Phys. Rev. **123**, 1326 (1961).
- [11] A. Arima, H. Horie, Progr. Theoret. Phys. (Kyoto) **12**, 623 (1954); H. Noya, A. Arima, H. Horie, Progr. Theor. Phys. (Kyoto) **8**, Supplement, 33 (1958).
- [12] E.-W. Otten, Some recent developments in laser spectroscopy of unstable nuclei, *4th International conference on nuclei far from stability*, CERN yellow report 81-09, Vol. I, 20 July 1981, 3; *Nuclei Far from Stability*, edited by D.A. Bromley, *Treatise on Heavy Ion Physics* **8** (Plenum, New York, 1989) 517.

- [13] E. Fermi, *Z. Phys.* **60**, 320 (1930); E. Fermi and E.G. Segrè, *Z. Phys.* **82**, 729 (1933).
- [14] H.H. Stroke *et al.*, *Phys. Rev.* **105**, 590 (1957).
- [15] J.S. Grossman *et al.*, *Phys. Rev. Lett.* **83**, 935 (1999).
- [16] J.R. Persson, *Eur. Phys. J. A* **2**, 3 (1998).
- [17] S. Millman, I.I. Rabi, and J.R. Zacharias, *Phys. Rev.* **53**, 384 (1938).
- [18] ISOLDE website [http://isolde.yields with synchrocyclotron \(SC\)](http://isolde.yields.withsynchrotron.com)
- [19] C. Thibault *et al.*, *Phys. Rev. C* **23**, 2720 (1981).
- [20] F. Touchard *et al.*, *Nucl. Instrum. Methods* **186**, 329 (1981).
- [21] T. Dinneen, A. Ghiorso, H. Gould, *Rev. Sci. Instrum.* **67**, 752 (1996).
- [22] David A. Dahl, *Simion 3D, 6.0* (Bechtel BWXT IDAHO, LLC, 2000) (D.A. Dahl, MS 2208, Idaho National Engineering and Environmental Laboratory, POB 1625, Idaho Falls, ID 83415).
- [23] N.F. Ramsey, *Molecular Beams* (Clarendon Press, Oxford, 1956), Equation V.10.
- [24] C. Thibault *et al.*, *Nucl. Phys.* **A367**, 1 (1981).
- [25] C. Ekström *et al.*, *Nucl. Phys. A* **292**, 144 (1977).
- [26] S. Trapp *et al.*, *Hyperfine Interactions* **127**, 57 (2000).

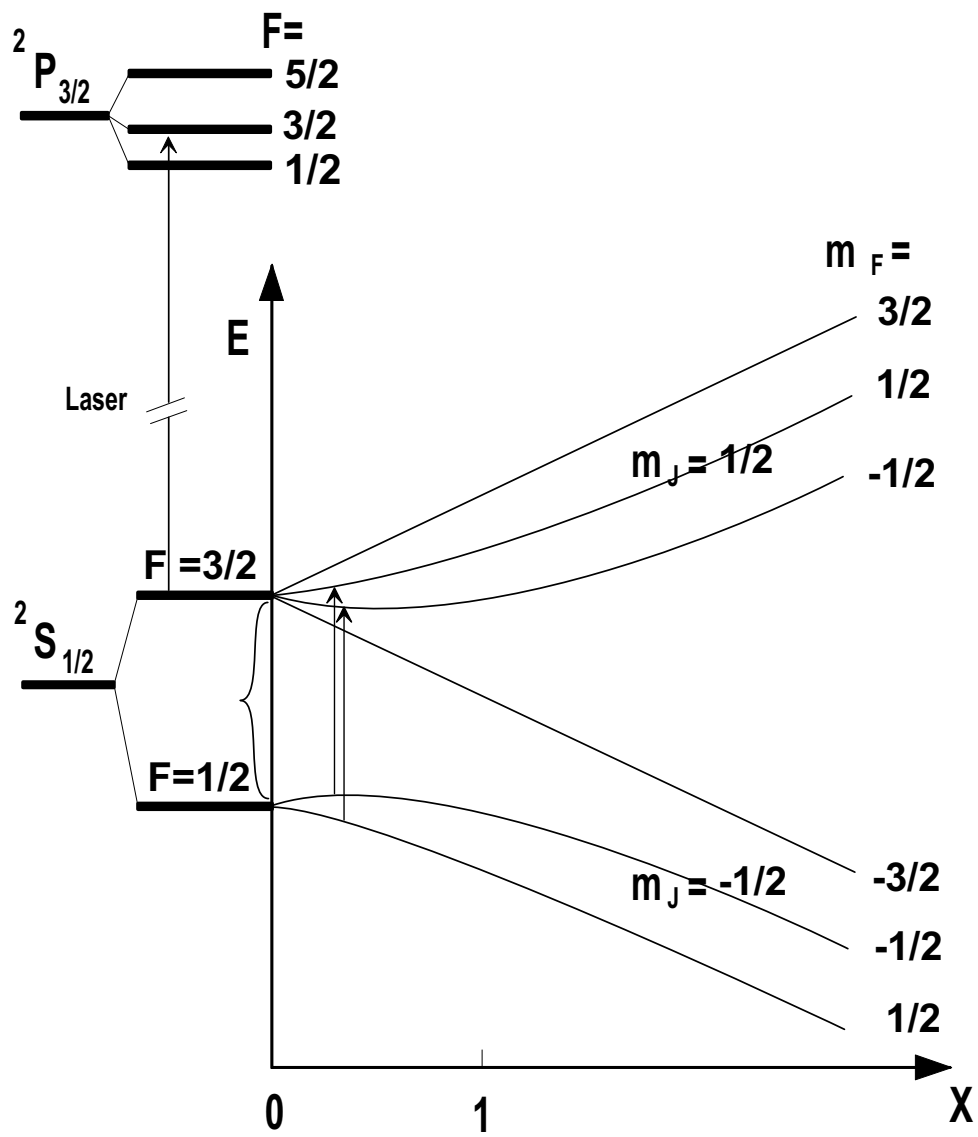


Figure 1: Zeeman effect of the hfs of ^{126}Cs . The measured, nearly field-independent, transitions are shown.

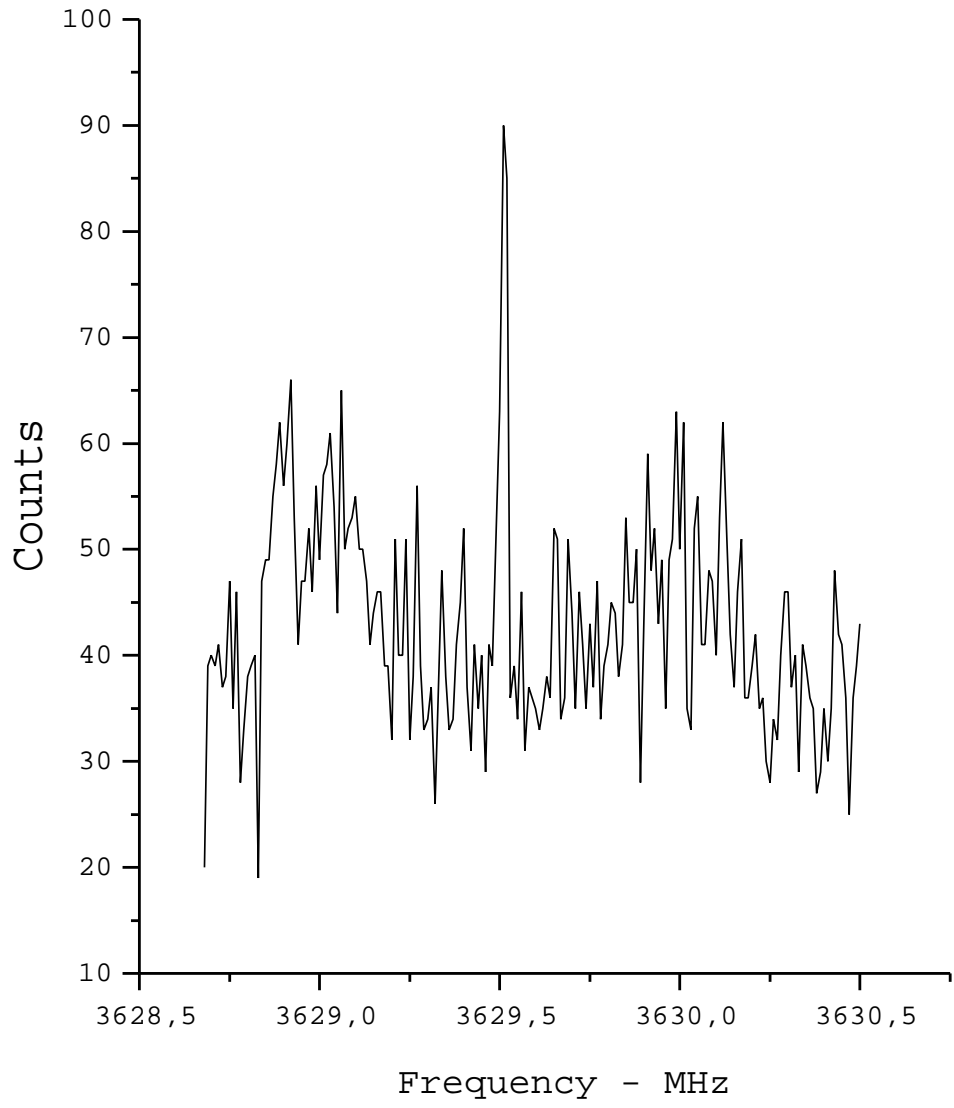


Figure 2: ^{126}Cs hfs field-dependent and -independent transitions: 10 kHz per step, 5-s integration time.

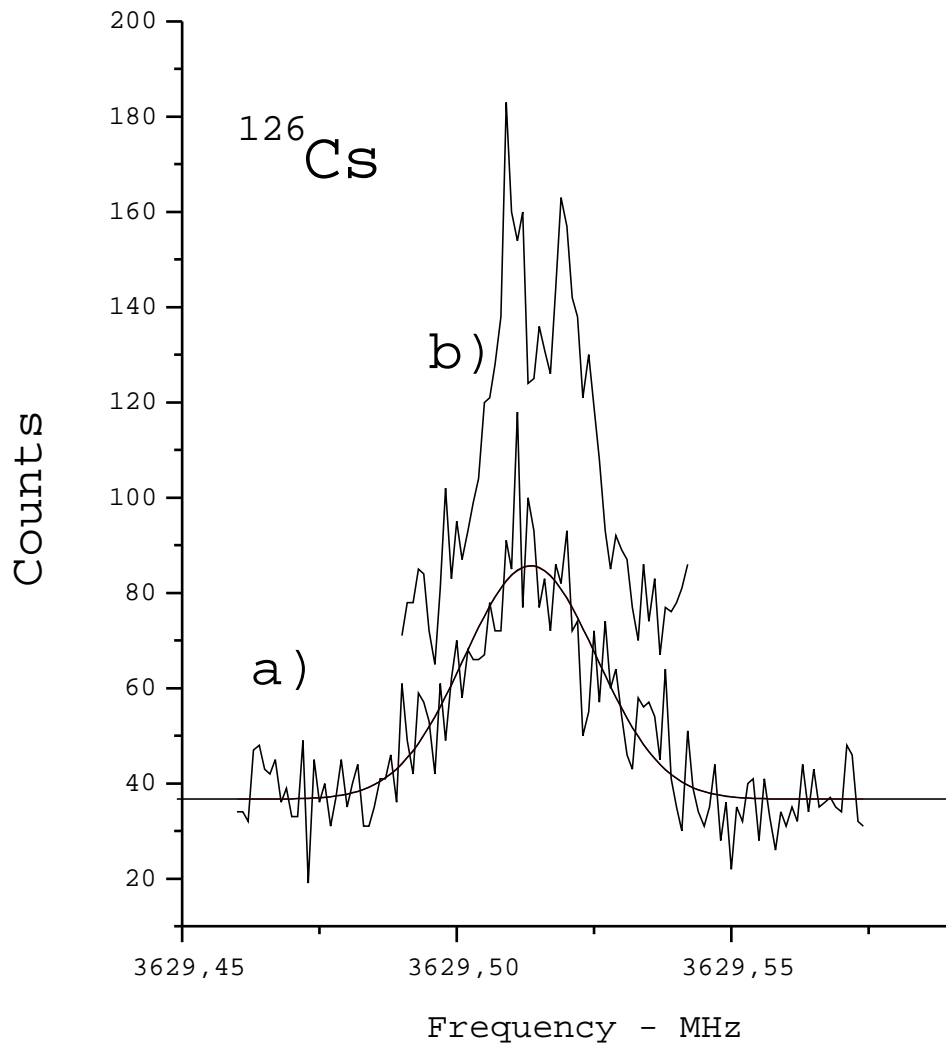


Figure 3: ^{126}Cs [F, m_F ($1/2, 1/2$) \rightarrow ($3/2, -1/2$) and ($1/2, -1/2$) \rightarrow ($3/2, 1/2$)] superposed hfs components: 10 kHz per step; (a) 5-s integration time, (b) 10-s integration time at half the rf power.